

## UNRAVELING THE 10 MICRON “SILICATE” FEATURE OF PROTOSTARS: THE DETECTION OF FROZEN INTERSTELLAR AMMONIA

J. H. LACY AND H. FARAJI

Department of Astronomy, University of Texas, Austin, TX 78712

AND

S. A. SANDFORD AND L. J. ALLAMANDOLA

NASA Ames Research Center, MS 245-6, Moffett Field, CA 94035-1000; ssandford@mail.arc.nasa.gov

Received 1998 March 19; accepted 1998 May 5; published 1998 June 18

### ABSTRACT

We present infrared spectra of four embedded protostars in the 750–1230  $\text{cm}^{-1}$  (13.3–8.1  $\mu\text{m}$ ) range. For NGC 7538 IRS 9, a new band is reported at 1110  $\text{cm}^{-1}$  (9.01  $\mu\text{m}$ ), and several others may be present near 785, 820, 900, 1030, and 1075  $\text{cm}^{-1}$  (12.7, 12.2, 11.1, 9.71, and 9.30  $\mu\text{m}$ ). The band at 1110  $\text{cm}^{-1}$  is attributed to frozen  $\text{NH}_3$ . Its position and width imply that the  $\text{NH}_3$  is frozen in a polar,  $\text{H}_2\text{O}$ -rich interstellar ice component. The  $\text{NH}_3/\text{H}_2\text{O}$  ice ratio inferred for NGC 7538 IRS 9 is 0.1, making  $\text{NH}_3$  as important a component as  $\text{CH}_3\text{OH}$  and  $\text{CO}_2$  in the polar ices along this line of sight. At these concentrations, hydrogen bonding between the  $\text{NH}_3$  and  $\text{H}_2\text{O}$  can account for much of the enigmatic low-frequency wing on the 3240  $\text{cm}^{-1}$  (3.09  $\mu\text{m}$ )  $\text{H}_2\text{O}$  interstellar ice band. The strength of the implied  $\text{NH}_3$  deformational fundamental at 1624  $\text{cm}^{-1}$  (6.158  $\mu\text{m}$ ) can also account for the absorption at this position reported by ISO.

*Subject headings:* comets: general — ISM: abundances — ISM: clouds — ISM: molecules — infrared: ISM: lines and bands

### 1. INTRODUCTION

Mid-infrared spectra of embedded protostellar objects have shown that mixed-molecular ices, organic materials, and silicates are ubiquitous in dense clouds (see Sandford 1996). The ices play significant roles in cloud chemistry (see Charnley 1997) and in determining the chemical makeup and evolution of the planetesimals, protoplanets, and comets produced during the protostellar nebulae phase (Thomas et al. 1996). Great strides have been made in our knowledge of the ices during the past 20 years (see Sandford 1996; Whittet et al. 1996a; Allamandola et al. 1997 and references therein). However, of the most abundant, reactive, atomic species present after hydrogen (carbon, nitrogen, and oxygen), only the disposition of carbon is reasonably well understood in dense clouds. The principle reservoirs of oxygen and nitrogen remain unknown. There is significant, but indirect, evidence that most of the nitrogen is in the very stable, unreactive molecular form of  $\text{N}_2$ , and that much of the oxygen is in  $\text{O}_2$  (Elsila, Allamandola, & Sandford 1997; Ehrenfreund et al. 1997). More refractory materials, in the form of aromatic-rich dust (Sellgren et al. 1995), microdiamonds (Allamandola et al. 1992), and silicates (Willner et al. 1982), are also present in these clouds. Of these, the silicates have been longest known, but a complete understanding of their exact nature has proven elusive (see Tielens 1990). It has long been recognized that one of the difficulties inherent in the analysis of the “10  $\mu\text{m}$ ” feature in terms of silicates alone was the fact that this band is overlapped by absorptions caused by other materials (see, e.g., Allamandola & Sandford 1988). Here we reconsider the spectral region from 750 to 1230  $\text{cm}^{-1}$  toward four embedded objects in light of our current understanding of dense molecular clouds.

### 2. OBSERVATIONS

We observed four infrared sources embedded in molecular clouds, W3 IRS 5, W33A, NGC 7538 IRS 1, and NGC 7538 IRS 9, in the 750–1230  $\text{cm}^{-1}$  (13.3–8.1  $\mu\text{m}$ ) region. The ob-

servations were made with the Irshell spectrograph (Lacy et al. 1989; Achtermann 1994) at the NASA IRTF on the nights of 1992 August 18–20 (UT). A 75 lines  $\text{mm}^{-1}$  grating was used in first-order, and a focal reduction lens was placed in front of the detector to give a spectral sampling of  $\Delta\lambda \approx 0.0045 \mu\text{m}$  ( $\Delta\nu \approx 0.45 \text{ cm}^{-1}$  at 10  $\mu\text{m}$ ), a spectral resolution of  $\Delta\lambda \approx 0.01 \mu\text{m}$  ( $\Delta\nu \approx 1.0 \text{ cm}^{-1}$  at 10  $\mu\text{m}$ ), and a spectral coverage at each grating setting of  $\Delta\lambda \approx 0.29 \mu\text{m}$ . To cover the entire 750–1230  $\text{cm}^{-1}$  region, many overlapping spectra were measured. Typically 10 s was spent on-source at each grating setting, during which time the source was nodded between two positions along the entrance slit. After each source observation, a blackbody calibrator and blank sky were observed, the grating angle was stepped to shift the spectrum by 0.025  $\mu\text{m}$ , and then the sequence was repeated. Because of the large overlap between spectra, each spectral point was observed 11 times, giving a total integration time per point of approximately 2 minutes. A visible guide star and the spectrally summed infrared signal were used for guiding.

The data were reduced with SNOOPY (Achtermann 1992). For each grating setting, spectra were extracted from the two nod positions and combined, followed by flat-fielding using the blackbody spectrum. These spectra were patched together after shifting based on atmospheric emission features and scaling based on comparison with overlapping spectra. Atmospheric features were sufficiently strong to allow precise and unambiguous spectral alignment, but flux scaling to correct for guiding, seeing, and focus changes was more problematical for several reasons. First, the flat-fielded spectra typically showed a spurious tilt, leading to a systematic change in the scaling factor, apparently resulting from a different illumination of the spectrograph by the blackbody and the sources. This effect was corrected by multiplying the spectra by a slope function before patching them together. However, the spectral slope changed whenever the telescope or spectrograph focus was changed, which was necessary to correct for thermal and chromatic focus shifts. Consequently, spurious broad spectral features appear

in the spectra near wavelengths in which focus corrections occurred. In particular, apparent broad features centered near  $900\text{--}950\text{ cm}^{-1}$  ( $11.1\text{--}10.5\text{ }\mu\text{m}$ ) can be due in part to focus shifts made near that wavelength. The source spectra were divided by spectra of Capella ( $\alpha\text{ Aur}$ ), measured in the same way, to correct for atmospheric absorption features and to improve the correction for instrumental features that were not completely removed by flat-fielding.

The spectra of W3 IRS 5, W33A, NGC 7538 IRS 1, and NGC 7538 IRS 9 are shown in Figure 1. The W3 IRS 5 spectrum is incomplete owing to observing time limitations, and no data were obtained from W33A between  $990$  and  $1060\text{ cm}^{-1}$  ( $10.1$  and  $9.4\text{ }\mu\text{m}$ ) as a result of the strong interstellar silicate and telluric ozone absorption in this region. All spectra are dominated by the interstellar "silicate" absorption feature, which is centered at  $1030\text{ cm}^{-1}$  ( $9.7\text{ }\mu\text{m}$ ) but extends across the entire  $750\text{--}1230\text{ cm}^{-1}$  ( $13\text{--}8\text{ }\mu\text{m}$ ) region. The spectra are noisier near their ends, where the atmospheric transmission is poor. They are also noisier near  $1030\text{ cm}^{-1}$  because the fluxes are considerably lower in the center of the absorption band and because telluric  $\text{O}_3$  has a strong feature at this position.

The spectrum of NGC 7538 IRS 9 shows clear evidence for a discrete absorption near  $1110\text{ cm}^{-1}$ , as well as possible bands near  $900$  (very broad; nearly  $150\text{ cm}^{-1}$  total width),  $1030$ , and  $1075\text{ cm}^{-1}$ . Substantially weaker  $1110\text{ cm}^{-1}$  features may be seen toward W3 IRS 5 and NGC 7538 IRS 1, and there may be strong absorption here toward W33A, although our inability to detect this source at frequencies lower than  $1075\text{ cm}^{-1}$  make this uncertain (see § 3). NGC 7538 IRS 9 also shows weak, but probably real, absorptions near  $785$  and  $820\text{ cm}^{-1}$ . Because of the weakness of the  $785$  and  $820\text{ cm}^{-1}$  features and the uncertainty of the  $900$ ,  $1030$ , and  $1075\text{ cm}^{-1}$  features, we will largely restrict our discussion to the clearly present feature at  $1110\text{ cm}^{-1}$  in NGC 7538 IRS 9.

### 3. FROZEN AMMONIA ( $\text{NH}_3$ )

Submillimeter observations have shown that  $\text{NH}_3$  is one of the most abundant gas-phase molecules in dense clouds (see Cesaroni et al. 1994) where models suggest that  $\text{NH}_3$  should be formed in the gas phase (see Scott, Freeman, & McEwen 1997). At the low temperatures typical of dense clouds ( $T < 50\text{ K}$ ),  $\text{NH}_3$  should freeze onto grains very efficiently (Sandford & Allamandola 1993). The presence of solid state  $\text{NH}_3$  is implied by the fact that gas phase  $\text{NH}_3$  is enhanced in warmer cloud regions, where it is posited to be subliming from ices (see Cesaroni et al. 1994).

In the solid phase,  $\text{NH}_3$  possesses three vibrational fundamentals that are infrared active—a strong NH stretch at  $3450\text{ cm}^{-1}$  ( $2.90\text{ }\mu\text{m}$ ), a moderately strong NH deformation at  $1624\text{ cm}^{-1}$  ( $6.158\text{ }\mu\text{m}$ ), and a strong inversion mode near  $1100\text{ cm}^{-1}$  ( $9.10\text{ }\mu\text{m}$ ) that is very sensitive to interactions of the  $\text{NH}_3$  with neighboring molecules (d'Hendecourt & Allamandola 1986).

None of these bands have been conclusively observed in interstellar spectra. The NH stretch, which overlaps the strong OH stretching bands of  $\text{H}_2\text{O}$  and alcohols near  $3250\text{ cm}^{-1}$  ( $3.08\text{ }\mu\text{m}$ ), has received the most attention. It was shown in the first paper to compare ice analog spectra with interstellar spectra that if  $\text{NH}_3$  was frozen in interstellar ices it would produce absorption near  $3450\text{ cm}^{-1}$  ( $2.90\text{ }\mu\text{m}$ ), and it was suggested that this might account for spectral structure observed toward several objects (Hagen, Allamandola, & Greenberg 1980). This band was subsequently sought unsuccessfully (see Knacke et al. 1982) and it has been argued that scattering might also

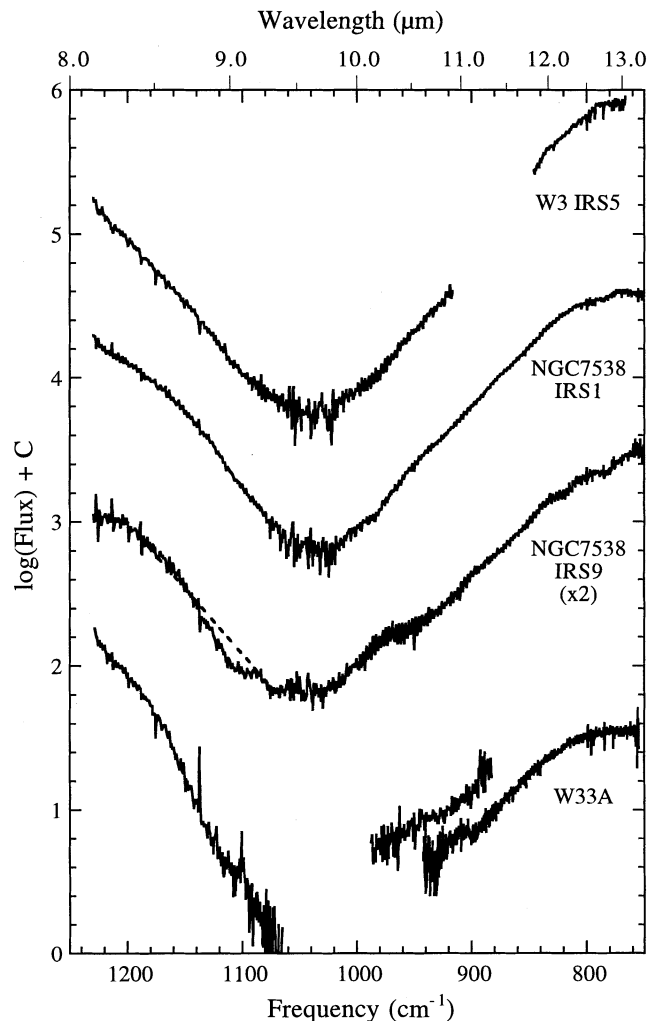


FIG. 1.—Infrared flux (on a logarithmic scale with arbitrary offsets) between about  $750$  and  $1230\text{ cm}^{-1}$  measured toward W3 IRS 5, NGC 7538 IRS 1, NGC 7538 IRS 9, and W33A. The dashed line between  $1070$  and  $1185\text{ cm}^{-1}$  on the spectrum of NGC 7538 IRS 9 represents the baseline used to derive the optical depth profiles in Figs. 2 and 3. The log (flux) numbers for NGC 7538 IRS 9 have been scaled by a factor of 2 to give the silicate feature a depth similar to the other sources.

produce structure at this position (Knacke & McCorkle 1987; Pendleton, Tielens, & Werner 1990). Most recently Whittet et al. (1996b) searched for this feature in the spectrum of HH 100-IR but were unable to confirm an earlier report of a clear absorption at this frequency (Graham & Chen 1991). The  $\text{NH}_3$  deformation mode at  $1624\text{ cm}^{-1}$  ( $6.158\text{ }\mu\text{m}$ ) has avoided detection because of severe overlap with the  $1670\text{ cm}^{-1}$  ( $6.0\text{ }\mu\text{m}$ )  $\text{H}_2\text{O}$  bending mode band. This leaves the inversion mode, which is very sensitive to the solid state environment of the molecule and which suffers from overlap with the poorly defined silicate feature centered near  $1030\text{ cm}^{-1}$  ( $9.7\text{ }\mu\text{m}$ ).

Here we report the clear detection of the inversion mode of  $\text{NH}_3$  frozen in  $\text{H}_2\text{O}$ . The spectra presented in Figure 1 show a moderately broad absorption band between about  $1060$  and  $1160\text{ cm}^{-1}$  toward NGC 7538 IRS 9, and possibly toward the other sources, especially W33A. Since the data quality is best for NGC 7538 IRS 9 and the feature is most prominent in its spectrum, discussion will be largely restricted to this object. The main difficulty in determining the frequency and profile of this feature is in separating it from the underlying silicate

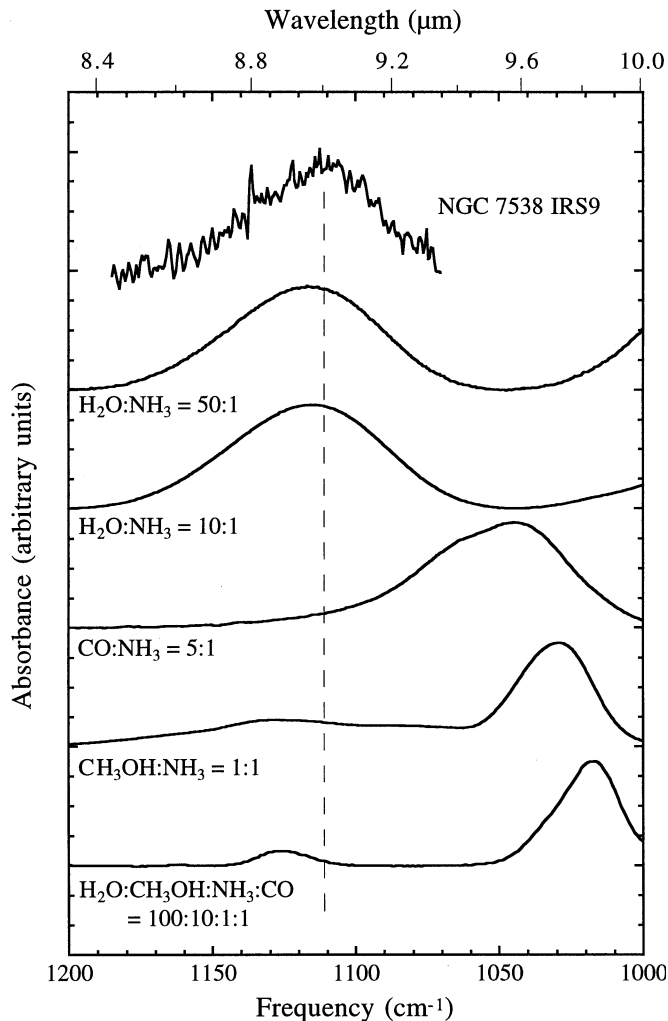


FIG. 2.—Absorbance spectra in the 1000–1200  $\text{cm}^{-1}$  region of several  $\text{NH}_3$ -containing mixed molecular laboratory ices compared to the 1110  $\text{cm}^{-1}$  feature seen toward NGC 7538 IRS 9. The interstellar feature was derived using the baseline shown in Fig. 1. The position and profile of the condensed interstellar ammonia inversion mode is well matched by  $\text{NH}_3$  frozen in an  $\text{H}_2\text{O}$ -rich ice.

absorption, whose intrinsic shape is not known. Several approaches were tried, including (1) drawing various straight or curved baselines on a plot of flux or log (flux) versus wavenumber, (2) calculating optical depth from the ratio of observed flux to the flux of a blackbody interpolated between the ends of the spectra and drawing various baselines on this plot, and (3) using either W3 IRS 5 or NGC 7538 IRS 1 as a silicate feature template to calculate the excess absorption toward NGC 7538 IRS 9. All four approaches gave essentially the same results for the position of the deepest absorption although they produced somewhat different widths and central depths, with the variations in strength being on the order of  $\pm 30\%$ . We adopted the straight baseline in log (flux) (Fig. 1), since it avoided the possibility of distortion of the spectrum by saturation, while making minimal assumptions about the underlying spectrum. We feel that this is the most conservative approach, since the intrinsic profile of the underlying silicate feature could be either concave, quasi-linear, or convex across the band.

Figure 2 compares the optical depth [ $\ln(I_0/I)$ ] of the feature produced with the baseline shown in Figure 1, which has  $\tau = 0.35$  and  $\text{FWHM} \approx 50 \text{ cm}^{-1}$  ( $\tau\Delta\nu = 17.5 \text{ cm}^{-1}$ ), to the laboratory spectra of  $\text{NH}_3$  frozen in several different ices. These

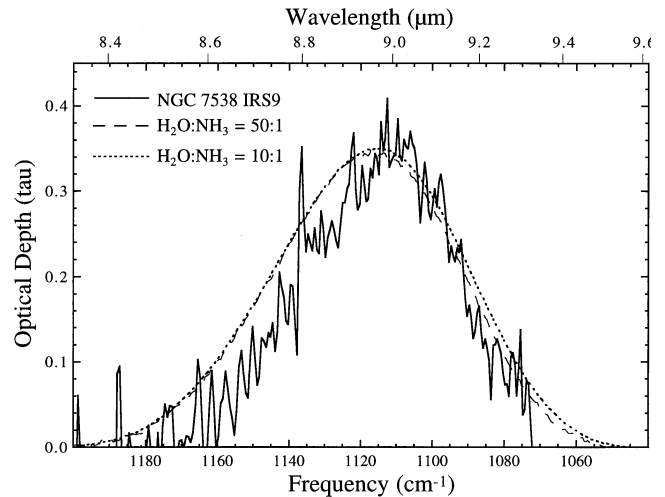


FIG. 3.—Interstellar 1110  $\text{cm}^{-1}$  band (in absorbance) toward NGC 7538 IRS 9 (solid line) compared with the  $\text{NH}_3$  inversion band produced by  $\text{H}_2\text{O}:\text{NH}_3 = 50$  (long-dashed line) and  $\text{H}_2\text{O}:\text{NH}_3 = 10$  (short-dashed line) ices at 10 K.

data demonstrate that this mode of frozen  $\text{NH}_3$  is highly sensitive to molecular environment. In the polar,  $\text{H}_2\text{O}$ -rich ice the feature falls at about 1115  $\text{cm}^{-1}$ , whereas in the nonpolar CO ice it shifts to 1045  $\text{cm}^{-1}$ . It is clear from these comparisons that the best match to the interstellar feature is provided by  $\text{NH}_3$  frozen in an  $\text{H}_2\text{O}$ -rich ice. Figure 3 shows a fit of  $\text{H}_2\text{O}:\text{NH}_3 = 50:1$  and  $10:1$  laboratory ice analogs to the interstellar feature. The fits are remarkably good and suggest that the band is caused by modest amounts of  $\text{NH}_3$  frozen in the  $\text{H}_2\text{O}$ -rich ices along this line of sight (LOS).

Laboratory spectra of ices containing methanol ( $\text{CH}_3\text{OH}$ ) are also shown in Figure 2, since it is present along the LOS to NGC 7538 IRS 9 (Allamandola et al. 1992). Methanol should produce a very strong band near 1025  $\text{cm}^{-1}$  (9.756  $\mu\text{m}$ ) and a moderately intense band near 1128  $\text{cm}^{-1}$  (8.865  $\mu\text{m}$ ) (Sandford & Allamandola 1993). While the 1128  $\text{cm}^{-1}$   $\text{CH}_3\text{OH}$  band does not provide a particularly good fit to the position or profile of the new 1110  $\text{cm}^{-1}$  interstellar band, it could contribute. The expected  $\text{CH}_3\text{OH}$  contributions to the spectrum at 1025 and 1128  $\text{cm}^{-1}$  can be calculated using the strength of the 2825  $\text{cm}^{-1}$  (3.54  $\mu\text{m}$ ) band of frozen  $\text{CH}_3\text{OH}$  toward NGC 7538 IRS 9 [ $\tau\Delta\nu(2825) = 3.64 \text{ cm}^{-1}$ ] (see Table 2 of Allamandola et al. 1992). Using the known relative strengths of the bands of  $\text{CH}_3\text{OH}$  in  $\text{H}_2\text{O}$ -rich matrices (Schutte, Tielens, & Sandford 1991; Hudgins et al. 1993), we would expect methanol to contribute  $\tau\Delta\nu = 7.28 \text{ cm}^{-1}$  at 1025  $\text{cm}^{-1}$  and  $\tau\Delta\nu = 1.12 \text{ cm}^{-1}$  at 1128  $\text{cm}^{-1}$ . Since the integrated strength of the observed 1110  $\text{cm}^{-1}$  feature is  $\tau\Delta\nu = 17.5 \text{ cm}^{-1}$ , the 1128  $\text{cm}^{-1}$  methanol feature can be contributing, at the very most, about 10% of the excess absorption in this spectral region. We therefore attribute the bulk of the 1110  $\text{cm}^{-1}$  absorption toward NGC 7538 IRS 9 to  $\text{NH}_3$  and not  $\text{CH}_3\text{OH}$ . As a related point, we note that the 1025  $\text{cm}^{-1}$  methanol band is typically about 10 times stronger than the one at 1128  $\text{cm}^{-1}$ . Thus, if methanol were responsible for the entire interstellar 1110  $\text{cm}^{-1}$  band, there would be a methanol band near 1025  $\text{cm}^{-1}$  in Figure 1 at least 10 times stronger than the possible weak feature actually observed near 1030  $\text{cm}^{-1}$  (see also Whittet et al. 1996a for another spectrum of NGC 7538 IRS 9).

Assuming that 90% of the excess absorption shown in Figure 2 is due to solid  $\text{NH}_3$  and using an intrinsic strength for the

1110  $\text{cm}^{-1}$  band of  $1.7 \times 10^{-17}$   $\text{cm molecule}^{-1}$  (d'Hendecourt & Allamandola 1986), we derive a frozen  $\text{NH}_3$  column density toward NGC 7538 IRS 9 of  $9.3 \times 10^{17}$   $\text{molecules cm}^{-2}$ . This column density exceeds those of solid  $\text{CH}_4$  and  $\text{CO}$  frozen in polar ices along this LOS ( $1.3 \times 10^{17}$  and  $3.2 \times 10^{17}$   $\text{molecules cm}^{-2}$ , respectively) and is comparable to those of frozen  $\text{CH}_3\text{OH}$  and  $\text{CO}_2$  ( $9.1 \times 10^{17}$  and  $1.2 \times 10^{18}$   $\text{molecules cm}^{-2}$ , respectively) (Allamandola et al. 1992; Boogert et al. 1996; de Graauw et al. 1996). The abundance of  $\text{H}_2\text{O}$  derived from the 1670  $\text{cm}^{-1}$  band along this same LOS (Tielens & Allamandola 1987) implies an  $\text{NH}_3/\text{H}_2\text{O}$  ice ratio of about 10%. This value is perfectly consistent with the ratios used in the laboratory ices shown in Figure 3, which provide a good fit to the interstellar 1110  $\text{cm}^{-1}$  feature's position and profile. Note that comets, whose abundances of other icy components are increasingly being found to be similar to those in dense clouds, show  $\text{NH}_3/\text{H}_2\text{O}$  values ranging from about 0.01% to 1.8% (Wycoff, Tegler, & Engel 1989; Feldman et al. 1993; Bird et al. 1997).

If one assumes that  $\text{NH}_3$  is present in the polar ice components along the LOS to the other three objects in Figure 1 in the same concentration with respect to  $\text{H}_2\text{O}$  as seen in NGC 7538 IRS 9, one predicts features about half the depth toward W3 IRS 5 and NGC 7538 IRS 1 and one several times larger toward W33A.  $\text{NH}_3$  features are not obviously present in the spectra of W3 IRS 5 and NGC 7538 IRS 1, but given the greater depths of their silicate features compared to NGC 7538 IRS 9 (note the different scale for IRS 9 in Fig. 1),  $\text{NH}_3$  features as deep as one-half that toward IRS 9 could well be present. In the spectrum of W33A, there is evidence of a distortion of the high-frequency side of the silicate feature consistent with  $\text{NH}_3$  absorption, but the lack of low-frequency baseline information makes it impossible to derive a depth of the  $\text{NH}_3$  feature.

The presence of  $\text{NH}_3$  has implications for other regions of the spectrum of NGC 7538 IRS 9. Based on a  $\tau$  of 0.31 for the  $\text{NH}_3$  contribution to the 1110  $\text{cm}^{-1}$  band, frozen  $\text{NH}_3$  should also produce absorptions near 3375  $\text{cm}^{-1}$  (2.96  $\mu\text{m}$ ) ( $\tau \sim 0.4$ ) and 1624  $\text{cm}^{-1}$  (6.158  $\mu\text{m}$ ) ( $\tau \sim 0.1$ ) (d'Hendecourt & Allamandola 1986; Sandford & Allamandola 1993). Detection of the 3375  $\text{cm}^{-1}$  band toward NGC 7538 IRS 9 is not possible because of saturation caused by the  $\text{H}_2\text{O}$  ice band (Allamandola et al. 1992). However, absorption centered near 1610  $\text{cm}^{-1}$  (6.21  $\mu\text{m}$ ) has been recently reported in the spectrum of NGC 7538 IRS 9 (Schutte et al. 1996). Schutte et al. attributed this band to aromatic materials, but we note that a significant fraction of the optical depth of this band ( $\tau \approx 0.1$ ) can be accounted for by  $\text{NH}_3$ . Nonetheless, as discussed by Schutte et al., baseline uncertainties could easily accommodate this and a contribution by aromatic material is reasonable.

The presence of  $\text{NH}_3$  also has important consequences for the low-frequency wing on the "3  $\mu\text{m}$ " interstellar  $\text{H}_2\text{O}$  ice

band (Allamandola 1984). Most (but not all) protostellar spectra contain  $\text{H}_2\text{O}$  ice bands that have an unexplained low-frequency wing with a strength between 10 and 15% that of the peak depth at 3240  $\text{cm}^{-1}$  (3.09  $\mu\text{m}$ ) (Smith, Sellgren, & Tokunaga 1989).  $\text{H}_2\text{O}:\text{NH}_3$  complexes produce such low-frequency wings with optical depths roughly 10% that of the maximum of the 3240  $\text{cm}^{-1}$  feature for  $\text{H}_2\text{O}:\text{NH}_3$  ratios of about 10/1 (Hagen, Tielens, & Greenberg 1983). Thus, if the  $\text{NH}_3/\text{H}_2\text{O}$  ratio of 0.1 we infer for NGC 7538 IRS 9 is typical of the LOS to protostellar objects, a significant fraction of the interstellar low-frequency wing on the 3240  $\text{cm}^{-1}$   $\text{H}_2\text{O}$  ice feature can be attributed to the strong hydrogen bonding between  $\text{NH}_3$  and  $\text{H}_2\text{O}$  as described in Allamandola (1984). Additional contributions in this region probably come from materials that contain  $sp^3$  type CH bonds such as chars (Smith et al. 1989), short aliphatic chains (Sandford et al. 1991), and diamond-like materials and methanol (Allamandola et al. 1992; Sellgren, Smith, & Brooke 1994; Brooke, Sellgren, & Smith 1996).

#### 4. CONCLUSIONS

We present infrared spectra of four embedded protostars in the 750–1230  $\text{cm}^{-1}$  range. NGC 7538 IRS 9 clearly shows a new band at 1110  $\text{cm}^{-1}$  (9.01  $\mu\text{m}$ ) and probable bands at 785, 820, 900, 1030, and 1075  $\text{cm}^{-1}$  (12.7, 12.2, 11.1, 9.71, and 9.30  $\mu\text{m}$ ). The band at 1110  $\text{cm}^{-1}$  is attributed to  $\text{NH}_3$  frozen in polar,  $\text{H}_2\text{O}$ -rich interstellar ices. The  $\text{NH}_3/\text{H}_2\text{O}$  ice ratio inferred for NGC 7538 IRS 9 is 0.1, making ammonia an important component of the polar ices along this LOS. Interactions between the  $\text{NH}_3$  and  $\text{H}_2\text{O}$  can account for much of the low-frequency wing on the 3240  $\text{cm}^{-1}$  (3.09  $\mu\text{m}$ )  $\text{H}_2\text{O}$  interstellar ice band. The strength of the implied  $\text{NH}_3$  deformation fundamental at 1624  $\text{cm}^{-1}$  (6.158  $\mu\text{m}$ ) must contribute significantly to the absorption at this position reported by ISO. The ammonia feature may be present in the spectra of the other protostars as well.

In conclusion, it is becoming increasingly apparent that the interstellar "10  $\mu\text{m}$  silicate" feature produced by the materials in dense clouds is a result of overlapping absorptions caused by a wide variety of materials, only some of which are actually silicates!

The authors wish to thank K. Luhman for assistance with the observations and J. M. Achtermann and M. J. Richter for assistance with the data reduction. This work was supported by NSF grant AST-9618723 and NASA grants 344-38-12-04 (Exobiology) and 344-37-44-01 (Origins of Solar Systems). This Letter benefited from the comments of an anonymous reviewer.

#### REFERENCES

- Achtermann, J. M. 1992, in ASP Conf. Ser. 25, *Astronomical Data Analysis Software and Systems*, ed. D. M. Worrall, C. Biemsderfer, & J. Barnes (San Francisco: ASP), 451
- . 1994, *PASP*, 106, 173
- Allamandola, L. J. 1984, in *Galactic and Extragalactic Infrared Spectroscopy*, ed. M. Kessler & P. Phillips (Dordrecht: Reidel), 5
- Allamandola, L. J., Bernstein, M. P., & Sandford, S. A. 1997, in *Astronomical and Biochemical Origins and the Search for Life in the Universe*, ed. C. B. Cosmovici, S. Bowyer, & D. Werthimer (Bologna: Edit. Comp.), 23
- Allamandola, L. J., & Sandford, S. A. 1988, in *Dust in the Universe*, ed. M. E. Bailey & D. A. Williams (Cambridge: Cambridge Univ. Press), 229
- Allamandola, L. J., Sandford, S. A., Tielens, A. G. G. M., & Herbst, T. M. 1992, *ApJ*, 399, 134
- Bird, M. K., Huchtmeier, W. K., Gensheimer, P., Wilson, T. L., Janardhan, P., & Lemme, C. 1997, *A&A*, 325, L5
- Boogert, A. C. A., et al. 1996, *A&A*, 315, L377
- Brooke, T. Y., Sellgren, K., & Smith, R. G. 1996, *ApJ*, 459, 209
- Cesaroni, R., Churchwell, E., Hofner, P., Walmsley, C. M., & Kurtz, S. 1994, *A&A*, 288, 903
- Charney, S. B. 1997, *MNRAS*, 291, 455
- d'Hendecourt, L. B., & Allamandola, L. J. 1986, *A&ASS*, 64, 453
- de Graauw, Th., et al. 1996, *A&A*, 315, L345
- Ehrenfreund, P., Boogert, A. C. A., Gerakines, P. A., Tielens, A. G. G. M., & van Dishoeck, E. F. 1997, *A&A*, 328, 649
- Elsila, J., Allamandola, L. J., & Sandford, S. A. 1997, *ApJ*, 479, 818
- Feldman, P. D., Fournier, K. B., Grinin, V. P., & Zvereva, A. M. 1993, *ApJ*, 404, 348
- Graham, J. A., & Chen, W. P. 1991, *AJ*, 102, 1405
- Hagen, W., Allamandola, L. J., & Greenberg, J. M. 1980, *A&A*, 86, L3
- Hagen, W., Tielens, A. G. G. M., & Greenberg, J. M. 1983, *A&ASS*, 51, 389

- Hudgins, D. M., Sandford, S. A., Allamandola, L. J., & Tielens, A. G. G. M. 1993, *ApJSS*, 86, 713
- Knacke, R. F., & McCorkle, S. M. 1987, *AJ*, 94, 972
- Knacke, R. F., McCorkle, S., Puetter, R. C., Erickson, E. F., & Krätschmer, W. 1982, *ApJ*, 260, 141
- Lacy, J. H., Achtermann, J. M., Bruce, D. E., Lester, D. F., Arens, J. F., Peck, M. C., & Gaalema, S. D. 1989, *PASP*, 101, 1166
- Pendleton, Y., Tielens, A. G. G. M., & Werner, M. W. 1990, *ApJ*, 349, 107
- Sandford, S. A. 1996, *Meteorities Planet. Sci.*, 31, 449
- Sandford, S. A., & Allamandola, L. J. 1993, *ApJ*, 417, 815
- Sandford, S. A., Allamandola, L. J., Tielens, A. G. G. M., Sellgren, K., Tapia, M., & Pendleton, Y. 1991, *ApJ*, 371, 607
- Schutte, W. A., Tielens, A. G. G. M., & Sandford, S. A. 1991, *ApJ*, 382, 523
- Schutte, W. A., et al. 1996, *A&A*, 315, L333
- Scott, G. B. I., Freeman, C. G., & McEwan, M. J. 1997, *MNRAS*, 290, 636
- Sellgren, K., Brooke, T. Y., Smith, R. G., & Geballe, T. R. 1995, *ApJ*, 449, L69
- Sellgren, K., Smith, R. G., & Brooke, T. Y. 1994, *ApJ*, 433, 179
- Smith, R. G., Sellgren, K., & Tokunaga, A. T. 1989, *ApJ*, 344, 413
- Thomas, P. J., Chyba, C. F., & McKay, C. P., eds. 1996, *Comets and the Origin and Evolution of Life* (New York: Springer)
- Tielens, A. G. G. M. 1990, in *From Miras to PN: Which Path for Stellar Evolution?*, ed. M. O. Mennessier & A. Omont (Gif-sur-Yvette: Editions Frontières), 186
- Tielens, A. G. G. M., & Allamandola, L. J. 1987, in *Physical Processes in Interstellar Clouds*, ed. G. E. Morrill & M. Scholer (Dordrecht: Reidel), 333
- Whittet, D. C. B., et al. 1996a, *A&A*, 315, L357
- Whittet, D. C. B., et al. 1996b, *ApJ*, 458, 363
- Willner, S. P., et al. 1982, *ApJ*, 253, 174
- Wyckoff, S., Tegler, S., & Engel, L. 1989, *Adv. Space Res.*, 9, 3169